

# PARTICLE MOTION IN A SEA OF EDDIES

CLAUDIA PASQUERO

*GPS, CALTECH, Pasadena, CA, USA,*

*claudia@gps.caltech.edu*

ANNALISA BRACCO

*ICTP, Trieste, Italy,*

*annalisa@ictp.trieste.it*

ANTONELLO PROVENZALE

*ISAC-CNR, Torino, and CIMA, Savona, Italy,*

*a.provenzale@isac.cnr.it*

JEFFREY B. WEISS

*PAOS, University of Colorado, Boulder, CO, USA,*

*jeffrey.weiss@colorado.edu*

## Abstract

As more high-resolution observations become available, our view of ocean mesoscale turbulence more closely becomes that of a “sea of eddies.” The presence of the coherent vortices significantly affects the dynamics and the statistical properties of mesoscale flows, with important consequences on tracer dispersion and ocean stirring and mixing processes. Here we review some of the properties of particle transport in vortex-dominated flows, concentrating on the statistical properties induced by the presence of an ensemble of vortices. We discuss a possible parameterization of particle dispersion in vortex-dominated flows, adopting the view that ocean mesoscale turbulence is a two-component fluid which includes intense, localized vortical structures with non-local effects immersed in a Kolmogorovian, low-energy turbulent background which has mostly local effects. Finally, we report on some recent results regarding the role of coherent mesoscale eddies in marine ecosystem functioning, which is related to the effects that vortices have on nutrient supply.

## 1. Introduction

The ocean transports heat, salt, momentum and vorticity, nutrients and pollutants, and many other material and dynamical quantities across its vast spaces. Some of these transport

processes are at the heart of the mechanisms of climate variability and of marine ecosystem functioning. In addition, a large portion of the available data on ocean dynamics are in the form of float and drifter trajectories. These provide a Lagrangian view of the ocean circulation which is not always easy to disentangle.

A proper consideration of the issues mentioned above, from climate variability to the reconstruction of the ocean circulation, requires the understanding, modelling and parameterization of oceanic transport processes. However, this task can be difficult, as ocean motions include a full spectrum of different scales, from the displacement of individual molecules to the general circulation at basin and planetary scales. At each scale, structured motions appear, and “eddies” populate the flow.<sup>1</sup> Of course, eddies at different scales behave differently, some of them are coherent objects,<sup>2</sup> such as mesoscale vortices, other are random eddies that live for short times, such as the whirls of three-dimensional turbulence. While short-lived eddies can sometimes be described by approaches based on turbulent cascades and random-Fourier-phase approximations, the long-lived coherent vortices usually lead to a break-up of the random-phase approximation.

Since a complete description of ocean motions at all scales is not feasible, a common approach consists in identifying a scale range of interest where we resolve the dynamics in the best possible way. Fluctuations on smaller scales are described as turbulence (of course, once we define something as “turbulence” this does not mean we have proceeded much in its understanding). Fluctuations at scales larger than those of interest are considered as boundary conditions, or large-scale forcings. Therefore, depending on the detail of knowledge of the mean flow and on the scale we work with, a given dynamical feature can either be included in the mean flow, or accounted for as one component of the turbulent behavior, or included in the boundary conditions. In this chapter, we shall focus on the dynamics of approximately two-dimensional mesoscale eddies, and on their effect on particle transport. Consistently, the term eddy will be used to refer to dynamical features characterized by strong potential vorticity anomalies that survive for several turnover times (typically, eddies of this kind survive for months to years), and which have a size of at least a few kilometers. In this sense, we are describing coherent eddies.

One of the reasons why we focus on these dynamical structures is that mesoscale eddies are widespread in the world oceans, and they account for a large portion of the ocean turbulent kinetic energy. Observations reveal the presence of rings in the Gulf Current and in the Agulhas Current (Olson and Evans 1986, Garzoli et al. 1999, Arhan et al. 1999), Meddies in the North

---

<sup>1</sup>Note that the term eddy refers to a wide variety of dynamical features in the ocean. It can stand for the low-frequency mesoscale variability (i.e. the medium-size fluctuations in the general circulation), for the mesoscale and sub-mesoscale coherent vortices (vortical motions at scales smaller than the internal Rossby radius of deformation, McWilliams 1985), or for a generic complicated motion in the presence of turbulence.

<sup>2</sup>Here, by coherent we mean a dynamical structure that lives for times that are much longer than a suitably defined local turbulence time.

Atlantic subtropical gyre (Richardson et al., 2000; Bower et al., 1997), abyssal vortices in the Brazil Basin (Richardson et al., 1994; Richardson and Fratantoni, 1999; Hogg and Owens, 1999; Weatherly et al., 2002) and in the Red Sea (Shapiro and Meschanov, 1991), and small vortices close to the regions of deep water formation (Gulf of Lyon: Testor and Gascard, 2003; Labrador Sea: Pickart et al., 1996). Mesoscale and sub-mesoscale eddies have radii that range from 5 km in the Gulf of Lyon (Testor and Gascard, 2003) to more than 100 km for Agulhas Current Rings (Garzoli et al. 1999, Arhan et al. 1999).

The presence of eddies is also revealed by Lagrangian data, in particular by floats undergoing looping trajectories. Depending on the geographical area where the floats are deployed, the fraction of floats undergoing looping trajectories (loopers), range from a few percent to almost fifty percent (Richardson, 1993).<sup>3</sup> It is to be noted that the number of observed looping trajectories remains low despite the effort of launching instruments in the core of a ring. For this reason, a direct census of the vortex population is difficult and the quantitative estimate of their statistical properties is questionable. Nevertheless, the available observations suggest that some oceanic regions are densely packed with vortices. Surface structures can be observed by satellite using infrared images (Hooker et al., 1995), or altimetric maps (Goni et al. 1997, Stammer, 1997; Isern-Fontanet et al., 2003). Subsurface structures are more difficult to measure, and their presence can be inferred thanks to the swirling motion of Lagrangian floats, or by measuring lenses of water with different biological, chemical, and/or physical characteristics respect to the surrounding water (such as the salty Meddies exiting from the Mediterranean at the Gibraltar Strait). With the assumption of homogeneity of the vortex distribution, Richardson (1993) has estimated the vortex population in the North Atlantic to be composed of about a thousand eddies. Recently, a method for estimating some of the statistical properties of the vortex population from the analysis of a few velocity time series has been proposed by Pasquero et al. (2002). This method is quite efficient in homogeneous conditions, but its extension to the inhomogeneous distributions typical of the ocean environment has still to be pursued.

A final comment concerns the fact that mesoscale structures affect the population dynamics of phyto- and zooplankton (for a general introduction of the interaction between ocean motions and marine ecosystem dynamics see the book by Mann and Lazier 1996). Coherent vortices are associated with secondary currents responsible for both horizontal and vertical fluxes of nutrients (e.g., Falkowski et al. 1991, McGillicuddy and Robinson 1997, McGillicuddy et al. 1998, Siegel et al. 1999, Martin and Richards 2001, Lévy, Klein and Tréguier 2001, Martin et al. 2002, Lévy 2003). The fact that the nutrient fluxes have a fine spatial and temporal detail, generated by the eddy field, has important consequences on primary productivity (Martin et al. 2002, Pasquero et

---

<sup>3</sup>A looper is a float that makes at least two consecutive loops. Note that only a part of the loopers are effectively located inside vortex cores: many of them are simply swirling around a vortex a few times, moving elsewhere afterwards.

al. 2004) and the horizontal velocity field induced by the eddies has been suggested to play an important role in determining plankton patchiness (e.g., Abraham 1998, Mahadevan and Campbell 2002, Martin 2003). Owing to their trapping properties, vortices can also act as shelters for temporarily less-favoured planktonic species (Bracco et al. 2000c). Overall, these considerations indicate that mesoscale and sub-mesoscale eddies are important agents in marine ecosystem dynamics.

## 2. The two-component view of mesoscale turbulence

In this contribution we shall advocate the view that ocean mesoscale turbulence can be pictured as a two-component fluid: a sea of coherent vortices immersed into a background turbulence that is quite Kolmogorovian.<sup>4</sup> This two-component viewpoint forms the basis of how we interpret Lagrangian (and Eulerian) measurements and how we infer flow properties from them. This issue has two facets: a direct problem, where we derive the properties of Lagrangian transport from the knowledge of a two-component Eulerian flow, and an inverse problem, where we try to obtain the structure and dynamics of the advecting flow from the knowledge of an ensemble of Lagrangian measurements. The latter is probably the most important of the two from an oceanographic perspective, but we cannot do the inverse problem without first understanding the direct problem. An important issue is how we identify the two components. Twenty years of two-dimensional and 3D quasigeostrophic turbulence research has shown, at least, that spectral analysis is not enough to identify the two components. The spectral viewpoint is local in Fourier space and global in physical space, while coherent vortices are characterized by vorticity distributions that are local in physical space, and thus they are non-local in Fourier space. In addition, the spectral representation of a coherent vortex does not lead to random Fourier phases, and thus the presence of coherent vortices generates significant phase correlations in the Fourier spectrum of the field. Any approach that assumes random Fourier phases is thus doomed to failure when applied to vortex-dominated flows.

Until now, the best way to identify vortices has found to be the direct identification by some vortex census algorithm based on the analysis of local vorticity patches in physical space. A variety of such methods exists (Benzi et al. 1987, Farge and Rabreau 1988, McWilliams 1990, Siegel and Weiss 1997, McWilliams et al. 1999, Farge et al. 1999); all of them require the knowledge of the full vorticity field. A simplified version of a vortex census, which requires the knowledge of just a few Eulerian time series and provides the gross features of the vortex statistics such as the vortex density and the average vortex size, has also been proposed (Pasquero et al., 2002).

---

<sup>4</sup>The statistical properties of the background turbulence have been discussed for example by Siegel and Weiss (1997), using the separation procedure provided by their vortex census method.

Although coherent vortices are local vorticity concentrations, their effects are non-local: The velocity field generated by a coherent vortex is non-local as it extends to large distances from the vortex center, well beyond the region where vorticity is significant. The range where the effect of the vortex on the velocity field is significant depends on the vortex shape and on the degree of baroclinicity: Barotropic vortices extend their influence to far distances, while baroclinic lenses (such as Meddies) have a shorter range of influence.<sup>5</sup> In terms of the velocity field (and particle dispersion), the two-component view of mesoscale turbulence should not be seen as a purely spatial decomposition of space into separate vortex and non-vortex areas, but rather as the superposition of two dynamical components which can simultaneously act at the same spatial position. Thus, even Lagrangian floats that are always outside vortices could be significantly influenced by vortex dynamics.

In the following, we explore some of the Lagrangian implications of the two-component nature of mesoscale turbulence in the ocean. We discuss some of the properties of the vortex components, such as the role that vortices play as transport barriers and the properties of the velocity field that they induce. After this, we shall exploit the two-component nature of these flows to construct a stochastic parameterization of Lagrangian dispersion in mesoscale turbulence.

### 3. Equations of motion

In this contribution we shall mainly be concerned with the behavior of Lagrangian tracers in simple dynamical models of ocean mesoscale turbulence. The description of the oceanic turbulent dynamics can be simplified by considering that diapycnal motion is inhibited by the stable density stratification present in most regions of the ocean. We can think of a stratified, hydrostatic fluid as a stack of infinitesimally thin layers. The dynamics in each layer can be described by the quasi-geostrophic (QG) approximation (Pedlosky, 1987, Salmon, 1998), which refers to a slowly evolving layer of homogeneous, incompressible fluid in a rotating environment. With the further assumption that the fluid is inviscid, the equations of motion correspond to the conservation of potential vorticity, which in the QG approximation can be written as the sum of relative vorticity, planetary vorticity, and the contribution to potential vorticity due to variations in the layer thickness (vortex-tube stretching). The interesting characteristic of this model, from a mathematical point of view, is that potential vorticity is now a single scalar dynamical field that fully describes the dynamics. The model allows for the development of coherent structures but does not capture several features such as, for instance, the surfacing of isopycnals (Flierl, 1987). Barotropic models are a further simplification, that can be obtained from the QG approximation

---

<sup>5</sup>The Green's function associated with a barotropic (point) vortex decreases proportionally to  $\log(r)$ , where  $r$  is the distance from the core of the vortex. For a baroclinic (point) vortex, the Green's function goes as  $1/r$ . Therefore barotropic vortices extend their influence to far distance, while baroclinic vortices have a shorter range of influence (Bracco et al. 2004).

by discarding the effects of the stratification. Two-dimensional turbulence results from neglecting the effects of vortex-tube stretching. For a detailed description of these approximations see, e.g., Pedlosky (1987) and Salmon (1998). Note, also, that although barotropic and baroclinic QG turbulence have different Eulerian characteristics, they nevertheless lead to very similar particle dispersion processes (Bracco et al. 2004).

The Lagrangian equation of motion for an individual fluid particle moving in a two-dimensional flow is

$$\frac{d\mathbf{X}_i}{dt} = \mathbf{U}_i(t) = \mathbf{u}(\mathbf{X}_i(t), t) \quad (1)$$

where  $\mathbf{X}_i(t)$  and  $\mathbf{U}_i(t)$  are the position and velocity of the  $i$ -th particle, and  $\mathbf{u}$  is the Eulerian velocity at the particle position. Note that in this equation we do not equate force to mass times particle acceleration, but rather particle velocity to the velocity of the flow. This happens because the particle is assumed to have negligible size and vanishing inertia with respect to the advecting fluid, i.e., to be a fluid element. When particles have finite size and/or non-vanishing inertia, the equations of motion become more complicated, see e.g. Provenzale (1999) and Babiano et al. (2000) for a discussion of the dynamics of inertial and finite-size particles in vortex-dominated flows. In the following, we shall only consider the dynamics of fluid particles for which equation (1) holds.

#### 4. Mesoscale vortices as transport barriers

Lagrangian observations indicate that floats deployed inside a mesoscale vortex stay inside the eddy for a long time, undergoing a looping trajectory (Olson 1991, Richardson 1993, Garzoli et al. 1999, Richardson et al. 2000). Numerical simulation of barotropic and of baroclinic (stratified) quasi-geostrophic turbulence and of point-vortex systems confirm that the cores of coherent vortices are associated with islands of regular (non chaotic) Lagrangian motion that trap particles for times comparable with the vortex lifetime (Babiano et al. 1994), and that vortices are characterized by a strong impermeability to inward and outward particle fluxes, see e.g. Provenzale (1999) for a review. Particles can have more complex behavior and can eventually migrate from inside to outside of a vortex or viceversa only when highly (and relatively rare) dissipative events take place, as the deformation of a vortex due to the interaction with a nearby vortex, or the formation of a filament.<sup>6</sup> For this reason, an initially inhomogeneous particle distribution becomes homogeneous only on a very long time scale, which is determined by the typical lifetime of the vortices rather than by the typical eddy turnover time of the individual vortices.

---

<sup>6</sup>An attempt to rationalize a disturbed vortex in terms of a wave-like perturbation superimposed on a regular steady object has recently showed that regular islands of motion in an otherwise chaotic sea characterize the Lagrangian behavior inside the perturbed vortex (Beron-Vera et al. 2004)

The trapping behavior of coherent vortices can be rationalized in terms of potential vorticity conservation. The most general definition of potential vorticity (PV) is  $\Pi = (\boldsymbol{\omega}_{\mathbf{a}} \cdot \nabla \eta) / \rho$ , where  $\boldsymbol{\omega}_{\mathbf{a}} = \boldsymbol{\omega} + 2\mathbf{\Omega}$  is absolute vorticity, given by the sum of relative and planetary vorticity,  $\rho$  is the density of the fluid, and  $\eta$  is entropy. Neglecting dissipation, fluid particles move conserving PV, i.e., we can write

$$\frac{D\Pi}{Dt} = 0. \quad (2)$$

where  $D/Dt$  is the material (Lagrangian) derivative, that represents the temporal variation following a fluid element <sup>7</sup>.

If surfaces of constant potential vorticity are known, then much is known about the motion of Lagrangian tracers. For this reason potential vorticity, despite the fact that its definition is not always intuitive and it cannot easily be measured in the ocean, is a quantity that can be of help in the understanding of Lagrangian motions. For oceanographic application, a useful approximation to potential vorticity is  $\Pi = \frac{\omega_a}{\rho} \frac{d\rho}{dz}$  (Pedlosky, 1987), where the scalar  $\omega_a$  is the vertical component of absolute vorticity. In this case, from the knowledge of the horizontal velocity and the vertical density profile, a map of potential vorticity can be drawn (Fratantoni et al. 1995).

A first consequence of potential vorticity conservation is that regions of strong PV gradients can act as transport barriers (McIntyre 1989). For an ideal fluid with irrotational external forcing PV is conserved. When some little dissipation and/or rotational forcing is acting on the fluid, as it usually happens, PV is not conserved. If the PV-changing effects are small, PV is quasi-conserved. This means that in regions where PV changes slightly, the particles will be able to shift from one PV surface to another. However, strong PV gradients are much more difficult to overcome, as the change in PV that the particle should achieve to climb (or descend) the gradient may be too large compared to the effect of the non-irrotational forcings and dissipation present in the system. As a result, strong PV gradients can act as transport barriers.

This is the main physical reason why intense jets, associated with strong PV gradients, can act as efficient barriers to transport. The same happens for isolated vortices (which can be thought of as jets wrapped on themselves): Vortex edges act as barriers to transport because vortices are regions of anomalous potential vorticity, usually embedded in a background where PV oscillates with low variance around some reference value. The vortex edges are therefore characterized by a large potential vorticity gradient, which fluid particles can rarely cross. Entrainment or detrainment of fluid particles from vortices more likely occurs during highly dissipative events

---

<sup>7</sup>We have now three time derivatives. The partial (Eulerian) derivative,  $\partial/\partial t$ , is the local time derivative of an Eulerian field, function of space and time. The material, or Lagrangian, derivative is the time derivative following the trajectory of the fluid element,  $D/Dt = \partial/\partial t + \mathbf{u} \cdot \nabla$ . The underline symbol,  $\underline{\cdot}$ , is introduced to discriminate two-dimensional vectors (no underline) from three-dimensional vectors. The total time derivative, such as that used on the left hand side of equation (1), is used when the dynamical variable depends only on time, as happens for the particle position.

(when potential vorticity is not conserved), and when vortices undergo structural changes and disruption, such as in vortex merging or during the ejection of filaments from the vortex core (see, e.g., de Steur et al. 2004 for the study of tracer leakage from modeled Agulhas rings).

## 5. Estimate of Lagrangian statistics

In studying Lagrangian data, we should distinguish between time averages taken along a particle trajectory and ensemble averages performed over a set of different particles. The two averages, in principle, can give rather different results. One of the reasons for this behavior is that Lagrangian particles can have a very long memory when coherent structures, whose lifetime is long compared to other time scales in the problem, are present. For instance, if a Lagrangian particle is initially released in the background turbulence outside vortex cores, it will move around without entering any of the vortex cores present in the turbulent flow, until, in a quite rare event such as the formation of a new vortex, the particle will get trapped inside a newly-forming vortical structure. From that moment on, the particle will stay inside the vortex for times comparable with the vortex lifetime.

The above example indicates that the temporal convergence of the statistical properties of a set of Lagrangian trajectories can take place on rather long timescales, related to the lifetime of the coherent structures. Of course, ensemble averages over a large number of homogeneously-distributed Lagrangian particles do not suffer from this problem and they usually give a more complete picture of the flow. This illustrates the fact that ergodicity (i.e., equivalence of time and ensemble averages) is reached only on very long times, if ever, for Lagrangian statistics of particles moving in vortex-dominated flows, as discussed by Weiss et al. (1998) for point vortices and by Provenzale (1999) and Pasquero et al. (2002) for the vortices of two-dimensional turbulence. In the case of ocean floats, usually one does not have access to a full ensemble of simultaneously-launched Lagrangian floats, and often a mixture of ensemble and time averages has to be employed. An interesting question, then, concerns the trade-off between the number of particles required to provide a meaningful picture of the flow (i.e., a correct estimate of the statistical properties of the flow) and the length of the trajectories. The larger the number of Lagrangian particles, the shorter the minimum length of the trajectories needed to describe the flow, but the exact balance depends on many factors, including the level of turbulence, the density and intensity of coherent structures, and the location where the Lagrangian probes are released. In such cases, the possible lack of ergodicity should be carefully evaluated when computing Lagrangian statistics. This issue has been discussed in some detail by Pasquero et al. (2002), together with the comparison between Lagrangian and Eulerian second-order statistics (i.e., spectra and decorrelation times).

Another delicate aspect related to the estimate of Lagrangian statistics is due to the (spatial and temporal) inhomogeneity of most ocean flows. A standard pre-analysis procedure is the spatial

and temporal binning of the data, motivated by the need to group together and average only those Lagrangian data which refer to similar values of the mean and eddy kinetic energy. In fact, analysing data coming from different statistical distributions, and/or very different values of the mean and eddy kinetic energy can lead to spurious results. In theory, the binning operation is a well defined procedure, and the bin size should in principle be reduced until the statistical properties in each bin converge (Poulain, 2001). This procedure assumes that the number of data is large enough to guarantee statistically significant results for small bin size. Unfortunately, in most cases the Lagrangian field data sets are not large enough. A compromise has to be achieved between the need for homogeneity and the requirement of statistical significance in each bin. If not properly performed, the binning procedure adopted to eliminate spatial and temporal inhomogeneities can lead to spurious results; see the discussion in Bracco et al. (2003).

## 6. Velocity statistics

Barotropic vortices influence the velocity field at large distances compared to their size. This influence is seen in the probability distribution function (PDF) of the velocity. At high Reynolds numbers, when vortices are intense and have sharp profiles, velocity pdfs in barotropic turbulence have non-Gaussian tails indicating that high velocities are more probable than would be the case for a Gaussian field (Bracco et al. 2000a, Pasquero et al 2001).<sup>8</sup>

This non-Gaussianity has been previously discussed in the context of point vortices, which can be thought of as a simplified model of vortex dominated flows at very large Reynolds number (Min et al. 1996, Jiménez 1996, Weiss et al. 1998). In this context it has been shown that small velocities have a Gaussian distribution but the PDF has a non-Gaussian tail which is related to the slow decay with distance of the velocity induced by a single vortex. Convergence to a Gaussian PDF is obtained only in systems with an extremely large number of vortices, orders of magnitude more than exist in the ocean (Weiss et. al 1998).

Float trajectories in the North Atlantic (Bracco et al. 2000b) and in the Adriatic Sea (Falco et al. 2000, Maurizi et al. 2004) indicate that velocity PDF are non Gaussian, see figure 1. Typically, they have larger kurtosis than a normal distribution: they have a Gaussian-like core and non-Gaussian tails for high velocities. Similar results have been found (Bracco et al. 2003) from midlatitude fluid particle trajectories along isobaric surfaces in a simulation of the Atlantic Ocean dynamics at high resolution (MICOM model, 1/12 of a degree). This similarity in velocity PDFs between float data, ocean GCMs, simplified turbulence models, and point vortex systems suggests that the non-Gaussian nature of the velocity PDFs is due to the vortex component of the mesoscale turbulence.

---

<sup>8</sup>We are here referring to either Eulerian or Lagrangian velocity PDFs under the assumption that Lagrangian particles sample the whole domain. In this case, in fact, Lagrangian velocity PDFs must converge to the Eulerian ones. See also the well-mixed condition in Thomson (1987).

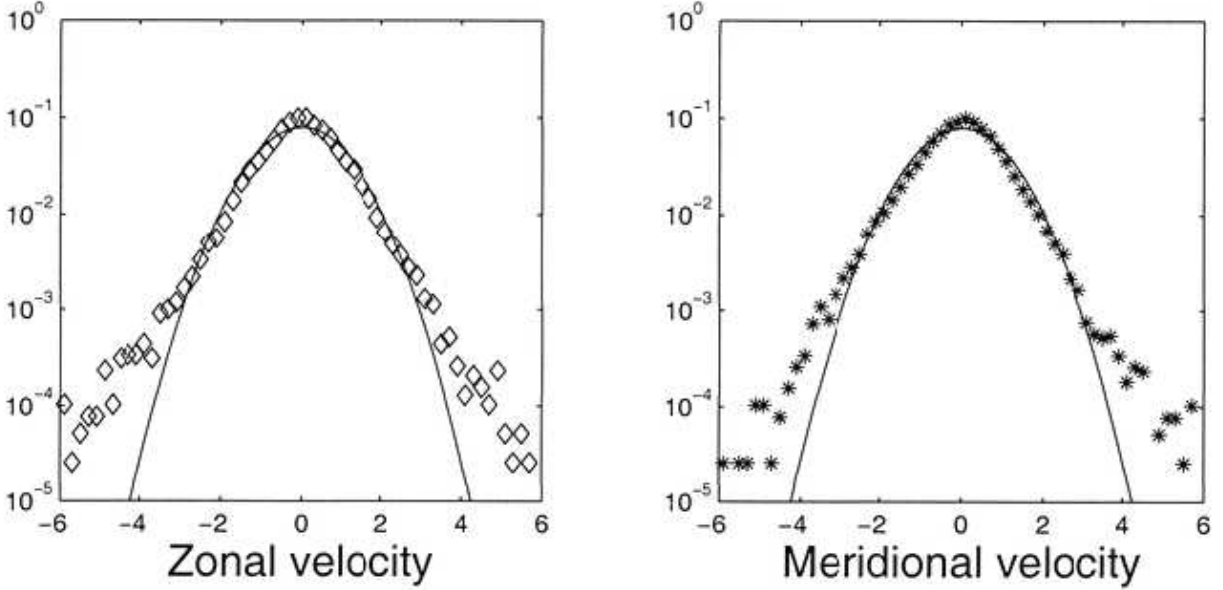


Figure 1: Velocity probability density function from floats in the deep Eastern North-Atlantic: (a) zonal component, (b) meridional component [from Bracco et al. 2000b].

Velocity distribution functions alone do not fully determine the characteristics of Lagrangian motion as they provide no information about velocity correlations. One important correlation is the memory a fluid parcel has of its past velocity, which is often characterized by the velocity autocorrelation function.

The single trajectory autocorrelation function for an individual particle (labelled by the index  $i$ ) is

$$R_i(\tau) = \frac{\overline{(\mathbf{U}_i(t) - \overline{\mathbf{U}}_i) \cdot (\mathbf{U}_i(t + \tau) - \overline{\mathbf{U}}_i)}}{\sigma_i^2}, \quad (3)$$

where  $\mathbf{U}_i(t)$  is the velocity of the  $i$ -th particle at time  $t$ ,  $\overline{\mathbf{U}}_i$  and  $\sigma_i^2$  are the mean and variance of the velocity of the  $i$ -th trajectory, and the overbar indicates an average over time  $t$ . Hence,  $R_i(0) = 1$  and  $R_i(\tau)$  goes to zero for large  $\tau$ , when the particle velocity loses memory of its initial value. The functions  $R_i(\tau)$  can be extremely different for different particles, depending on the dynamical characteristics of the region in which tracers move.

A particle trapped inside a vortex spins around the center of the vortex, which is itself advected by the flow. In this case,  $R_i$  is a decaying oscillatory function (see figure 2a). In other cases  $R_i$  can slowly decay with no oscillations, as in the case of a particle moving within a jet (Berloff et al. 2002). Point vortex systems show that long time correlations associated with high velocities occur in the vicinity of vortex pairs (Weiss et al. 1998), and there is indication that this behavior occurs in the ocean as well (Weatherly et al. 2002).

The flow field as a whole is characterized by the ensemble-averaged velocity autocorrelation function, defined by averaging over all trajectories. Because of the diversity of Lagrangian

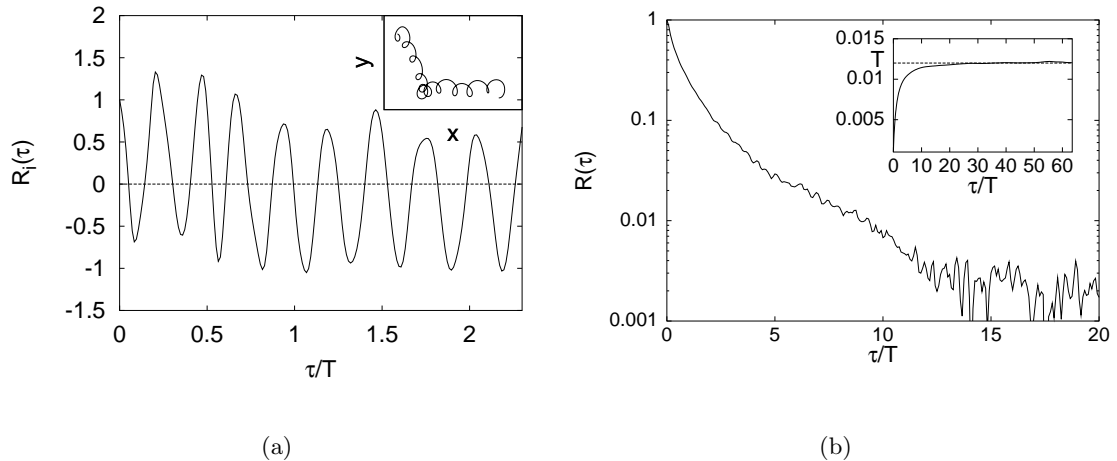


Figure 2: (a) Autocorrelation function,  $R_i(\tau)$ , for an individual particle moving within a vortex in a simulation of two-dimensional turbulence. The particle trajectory is shown in the inset. (b) Ensemble-averaged autocorrelation function,  $R(\tau)$ , for several thousand particles advected by two-dimensional turbulence. The inset shows the estimate of the Lagrangian integral time,  $T$ , as a function of the length of the trajectory [adapted from Pasquero et al. 2001].

histories which floats can experience, the estimate of ensemble-averaged autocorrelation functions is particularly sensitive to the typically small number of trajectories available in the ocean. Depending on the characteristics of coherent structures, the ensemble-averaged autocorrelation functions can also have oscillatory behavior (see Veneziani et al. 2004 for an example on float data).

One simple measure of the memory of Lagrangian particles is the Lagrangian integral time, defined as

$$T = \int_0^{\infty} R(\tau) d\tau. \quad (4)$$

When the autocorrelation function is exponential, the Lagrangian integral time is the decay time of the exponential,  $R(\tau) = e^{-\tau/T}$ . Typical values for  $T$  in the ocean are of the order of few days (Griffa et al. 1995, Garraffo et al. 2001, Zhang et al. 2001, Bauer et al. 2002).

## 7. Particle dispersion

Lagrangian particles in a Gaussian, homogeneous, stationary and uncorrelated velocity field undergo a Brownian random walk. Under such conditions, the second order moment of the distribution of particle displacements grows linearly with time:

$$A^2(\tau; t_0) \equiv \langle (\mathbf{X}_i(t_0 + \tau) - \mathbf{X}_i(t_0))^2 \rangle = 2K\tau \quad (5)$$

where  $K$  is the dispersion (or diffusion) coefficient. Here,  $\mathbf{X}_i(t)$  is the position of the  $i$ -th particle at time  $t$ , and the angular brackets denote an ensemble average over all particles. The function  $A^2(\tau, t_0)$  measures the absolute (or single-particle) dispersion. For a statistically stationary flow, the absolute dispersion  $A^2$  does not depend on the starting time  $t_0$ .

Relaxing any of the above assumptions (Gaussianity, homogeneity, stationarity, lack of temporal and spatial correlations) can significantly alter the dispersion law described above. On short time scales, in particular, the Brownian dispersion law is modified by the presence of spatial and temporal correlations in the advecting flow, which induce Lagrangian velocity correlations over a substantial time range. Over times much shorter than the Lagrangian integral time, the velocity is almost constant and one observes a ballistic dispersion phase,

$$A^2(\tau) = 2E\tau^2 \quad (6)$$

where  $E$  is the mean kinetic energy of the advecting flow.

A standard way of representing absolute dispersion is to define a time-dependent dispersion coefficient,  $K(\tau)$ , as

$$K(\tau) = \frac{A^2(\tau)}{2\tau} . \quad (7)$$

In the ballistic phase,  $K(\tau) \rightarrow E\tau$  as  $\tau \rightarrow 0$ , while in the Brownian dispersion phase  $K(\tau) \rightarrow K$  for  $\tau \rightarrow \infty$ . The ballistic regime is sometimes visible in the dispersion curves computed from surface drifter data (e.g. Colin de Verdiere, 1983). Subsurface float trajectories are often characterized by a well-defined ballistic regime, associated with very steep Lagrangian spectra at small times (Rupolo et al. 1996).

At long times, the presence of boundaries defines an upper saturation scale and it can destroy the Brownian behavior (Artale et al., 1997). Well before this, the presence of large-scale dynamical and geographical inhomogeneities and the temporal non-stationarity associated with different oceanic processes can also mask the Brownian dispersion phase. For example, meridional dispersion in the tropical Pacific Ocean has been found to depend on the strong wave activity typical of equatorial regions, which induces strong correlations in the acceleration (Bauer et al., 2002), and in the Adriatic Sea the diffusion coefficient computed from floats does not converge to a Brownian regime (Falco et al., 2000).

The analysis of float and drifter trajectories has also revealed the presence of anomalous dispersion regimes with  $K(\tau) \propto \tau^\alpha$  and  $\alpha \neq 0$  (Osborne et al. 1986, 1989, Sanderson and Booth 1991, Provenzale et al. 1991, Brown and Smith 1990). For example, in the analysis of surface drifter data in the Kuroshio extension region in the Pacific Ocean, Osborne et al. (1989) detected an anomalous dispersion regime with  $\alpha \approx 2/3$ . A power-law intermediate dispersion regime, albeit with a different exponent, has also been observed for two-dimensional barotropic turbulence and baroclinic quasi-geostrophic turbulence (Elhmaidi et al. 1993; Bracco et al. 2004). However, a satisfactory explanation of these anomalous regimes is lacking.

## 8. Parameterization of particle dispersion

Lagrangian stochastic models (LSM) are employed to reproduce the main statistical properties of particle trajectories in turbulent flows, without resolving the full Eulerian dynamics. Individual trajectories computed by a LSM usually do not have the same characteristics of the particles advected by a realistic flow. The similarity is recovered – if ever! – only statistically, after averaging over particle ensembles and over different realizations of the turbulent flow. Thus, one should not expect an individual stochastic trajectory to resemble an individual float trajectory. One simple class of stochastic models describes the process of single-particle dispersion. In this case, the spatial correlations of the advecting flow are discarded insofar as they do not translate into temporal correlations of the Lagrangian velocities (see also Rupolo et al. 1996 for a discussion of how Eulerian spatial correlations are related to Lagrangian time correlations). A more complex approach deals with particle separation processes, i.e., relative dispersion. In this case, the stochastic model describes the time evolution of the separation of a particle pair, and spatial correlations of the turbulent flow become an essential ingredient of the picture. In the following, we shall consider only single-particle dispersion and the related stochastic descriptions. An exhaustive discussion of the atmospheric applications of Lagrangian stochastic models can be found in Rodean (1996); for oceanographic applications see Griffa (1996) and Brickman and Smith (2002).

The simplest stochastic model for single-particle dispersion is the random walk (or Markoff-0 model). In this approach, the particle displacements are randomly extracted from a Gaussian distribution, and there is no temporal correlation between subsequent displacements. If we assume that there is no mean flow advecting the particles and that the turbulent flow is statistically isotropic, we can write a Lagrangian stochastic differential equation for the random walk as:

$$d\mathbf{X}_i = \sqrt{K} d\mathcal{W}_i(t). \quad (8)$$

where  $\mathbf{X}$  is the position of the  $i$ -th particle and the diffusivity,  $K$ , is not allowed to vary in space and time. The incremental Wiener random vector,  $d\mathcal{W}_i$ , has zero mean and it is  $\delta$ -correlated in space and time,  $\langle d\mathcal{W}_i(t) \cdot d\mathcal{W}_j(t') \rangle = \delta_{ij} \delta(t - t') dt$ .

The single-particle stochastic description illustrated above can be framed in terms of a deterministic partial differential equation for the time evolution of the probability density function of particle positions,  $P(\mathbf{X}|\mathbf{X}(0), t)$ . Defining the particle concentration at  $\mathbf{x}$  as  $C(\mathbf{x}, t) = \int P(\mathbf{X}=\mathbf{x}|\mathbf{X}(0), t) d\mathbf{X}(0)$ , the Fokker-Planck equation for the evolution of  $P$  gives the well-known diffusion equation:

$$\frac{\partial C(\mathbf{x}, t)}{\partial t} = \frac{1}{2} K \nabla^2 [C(\mathbf{x}, t)]. \quad (9)$$

The assumption of uncorrelated displacements is equivalent to the assumption that the Eulerian fluid velocities decorrelate instantaneously, i.e., that the turbulent structure of the flow has no

correlations. In general, this assumption is not appropriate for ocean mesoscale flows, where the temporal correlations of the advecting velocity field cannot be discarded. The simplest way of accounting for a memory in Lagrangian velocities is to consider a Markoff-1 model. In this approach, the time evolution of the Lagrangian velocity of the  $i$ -th particle,  $\mathbf{U}_i$ , is described by an Ornstein-Uhlenbeck process:

$$d\mathbf{U}_i = -\frac{\mathbf{U}_i}{T}dt + \sqrt{\frac{2\sigma^2}{T}}d\mathcal{W}_i. \quad (10)$$

where  $T$  is the Lagrangian correlation time and  $\sigma^2$  is the variance of the Lagrangian velocities. The first term on the r.h.s. is the (deterministic) fading-memory term, and the second term is the “stochastic kick”, or random component, of the velocity fluctuation. For this process, the velocity distribution is a Gaussian with zero mean and variance  $\sigma^2$ , and the velocity autocorrelation is an exponential,  $R(\tau) = \exp(-\tau/T)$ . The (time-dependent) diffusion coefficient can be computed analytically,

$$K(\tau) = \sigma^2 T \left[ 1 - \frac{T(1 - e^{-\tau/T})}{\tau} \right], \quad (11)$$

see Griffa (1996) for a discussion of this type of stochastic model in the context of oceanographic applications.

In a study of particle dispersion in two-dimensional turbulence, Pasquero et al. (2001) showed that the linear Ornstein-Uhlenbeck model provides a good representation of absolute dispersion at short and large times (respectively in the ballistic and Brownian regimes), while at intermediate times it provides estimates of the dispersion coefficient which differ by at most 25% from the values obtained by direct integration of particle dynamics in the turbulent flow. If this discrepancy is acceptable, due for example to uncertain or poorly resolved data, then the use of the Ornstein-Uhlenbeck model is sufficient. To obtain a more precise estimate of the dispersion coefficient, however, a stochastic model that more closely represents the processes of particle dispersion in vortex-dominated mesoscale turbulence is warranted.

Major differences between the Ornstein-Uhlenbeck process and particle dispersion in mesoscale turbulence are related to the facts that the velocity distribution is non-Gaussian (Bracco et al. 2000a), the velocity autocorrelation is non-exponential (Pasquero et al. 2001), and particles get trapped in vortices for long times (Elhmaidi et al. 1993, Babiano et al. 1994). Given these differences, it is indeed surprising that just a 25% discrepancy between the turbulent and the modelled dispersion coefficient is detected.

In an attempt to improve stochastic parameterizations of particle dispersion in mesoscale ocean turbulence, various extensions of the Ornstein-Uhlenbeck model have been proposed. The indications that Lagrangian accelerations in the ocean are correlated in time (Rupolo et al. 1996) have stimulated the development of Markoff-2 models where an Ornstein-Uhlenbeck formulation is written for the acceleration  $\mathbf{a}$ , with  $d\mathbf{U} = \mathbf{a} dt$  (e.g., Griffa 1996). Higher order models have

also been proposed, with the aim of better reproducing other statistical properties of Lagrangian motions such as the sub- or super-diffusive behavior at intermediate times (Berloff and McWilliams 2002). Superdiffusion has also been obtained by Reynolds (2002), using a variation of a Markoff-2 model that includes spin.

Models that include spin have been designed to explicitly describe particle motion in and around coherent structures. In the presence of coherent vortices, particle motion has a rotational component, as evident in the looping trajectories of floats deployed inside mesoscale eddies. The rotational component of the velocity vector along a Lagrangian trajectory is characterized by an acceleration orthogonal to the trajectory. Simple geometrical arguments show that the introduction of the spin in Markoff-1 models corresponds to adding a new term in the stochastic equation for the velocity increment, proportional to the orthogonal velocity component (Sawford 1999; Reynolds 2002). The individual trajectories produced by these models display spiralling motion, although the ensemble averaged velocity autocorrelation function is not necessarily oscillatory (Reynolds 2002). This model has recently been used to reproduce some statistical properties of Northwest Atlantic float trajectories (Veneziani et al. 2004).

On the other hand, it is not clear whether particle spinning inside vortices has any effect on space and time scales larger than those of the vortices themselves. In general, rotational motion inside vortices does not contribute to the large scale spreading of particles; it is only the motion of the vortex itself that is responsible for particle displacements at large scales. In turn, vortices move because they are advected by other vortices and there is no self-induction of the vortices themselves (Weiss et al. 1998). As a result, the large-time dispersion properties of Lagrangian particles inside or outside the vortices of two-dimensional turbulence are the same.<sup>9</sup> Thus, for the purpose of understanding particle dispersion at scales larger than the size of the individual vortices, the parameterization of particle motion inside a vortex can probably be neglected. In a study of single-particle dispersion in two-dimensional turbulence, Pasquero et al. (2001) proposed a parameterization of dispersion in two-dimensional turbulence at scales larger than those of the individual vortices. In doing so, no a priori difference between particles inside and outside vortices is drawn. The main point of the approach followed by Pasquero et al. (2001) is the observation that the Eulerian velocity at any point is determined by the combined effect of the far field of the vortices and the contribution of the local vorticity field in the background (Bracco et al. 2000a). Thus, even outside vortices, the velocity field induced by the coherent vortices cannot be discarded: on average, 80% of the kinetic energy in the background turbulence outside vortices is due to the velocity field induced by the vortex population. In addition, the non-Gaussian velocities measured in the background turbulence outside vortices are entirely due

---

<sup>9</sup>The situation is different on the  $\beta$ -plane, where vortices move differently with respect to fluid particles in the background turbulence. Here, significant differences between long-time dispersion properties of particles inside and outside vortices can be detected (Mockett 1998, Bracco et al., in preparation).

to the action of the surrounding vortices, which extend their influence far away from their inner cores. This is a signature of the non-locality of the velocity field: a particle moving in a vortex-dominated flow is heavily affected by the vortex dynamics even if it is not located inside them.

In this approach, the stochastic Lagrangian velocity of a particle at the position  $\mathbf{X}(t)$  is produced by the sum of two components,

$$\mathbf{U}(\mathbf{X}) = \mathbf{U}_B(\mathbf{X}) + \mathbf{U}_V(\mathbf{X}) , \quad (12)$$

where  $\mathbf{U}_B(\mathbf{X})$  is the velocity induced by the background turbulence and  $\mathbf{U}_V(\mathbf{X})$  is that induced by the vortices. The background-induced velocity is characterized by small energy and slow dynamics (i.e., long temporal correlations), while the vortex-induced component has large energy and it undergoes fast dynamics (whose temporal scale is of the order of the eddy turnover time). In addition, the vortex-induced component is characterized by a non-Gaussian velocity PDF. A different stochastic equation has then to be used for each of the two components. Since the background-induced velocity component,  $\mathbf{U}_B(\mathbf{X})$ , has a Gaussian distribution, a standard stochastic OU process can be used to describe it. As for the non-Gaussian, vortex-induced component  $\mathbf{U}_V(\mathbf{X})$ , a proper description is easily obtained by considering a nonlinear Markoff-1 model (Pasquero et al. 2001). In this case, one needs to consider a generalized Langevin equation

$$d\mathbf{U}_V = \mathbf{a}(\mathbf{U}_V)dt + b(\mathbf{U}_V)d\mathcal{W} \quad (13)$$

where the functions  $\mathbf{a}$  and  $b$  are functions of the velocity  $\mathbf{U}_V$ . The choice of the function  $\mathbf{a}(\mathbf{U}_V)$  is (not uniquely) determined by the corresponding Fokker-Planck equation, with the use of the well-mixed condition (Thomson 1987, Pasquero et al. 2001). In the end, the model proposed by Pasquero et al. (2001) becomes (we omit the particle index  $i$  for simplicity of notation):

$$\begin{aligned} d\mathbf{X} &= (\mathbf{U}_B + \mathbf{U}_V) dt \\ d\mathbf{U}_B &= -\frac{\mathbf{U}_B}{T_B}dt + \sqrt{\frac{2\sigma_B^2}{T_B}}d\mathcal{W}_B \\ d\mathbf{U}_V &= -\frac{2 + |\mathbf{U}_V|/\sigma_V}{(1 + |\mathbf{U}_V|/\sigma_V)^2} \frac{\mathbf{U}_V}{T_V} dt + \sqrt{\frac{2\sigma_V^2}{T_V}}d\mathcal{W}_V \end{aligned} \quad (14)$$

where  $T_B > T_V$ ,  $\sigma_V^2 \gg \sigma_B^2$ , and  $\mathcal{W}_B$  and  $\mathcal{W}_V$  are two independent Wiener processes.

Interestingly, the parameters of the stochastic model depicted above can be obtained from fits to an ensemble of Lagrangian trajectories (i.e., assuming no knowledge of the advecting velocity field). Comparison with particle advection in two-dimensional turbulence shows that this model captures single-particle dispersion with an error of less than 5%, and it does also capture statistical quantities measuring higher-order moments of the dispersion statistics (e.g., the distribution of first-exit times). Note that both the nonlinear nature of the vortex-induced

velocity and the presence of a low-energy background-induced velocity are essential ingredients of the model. At shorter times, the vortex-induced velocity dominates and it entirely determines statistical properties such as the non-Gaussian velocity distribution. At longer times, the vortex-induced velocity becomes rapidly uncorrelated and the lower-energy background-induced velocity gives a significant contribution to particle dispersion.

One advantage of the model illustrated above is that it has been built from a detailed knowledge of the dynamics of vortex-dominated flows. That is, it is not obtained by ignoring the structure of the flow, but from an attempt to reproduce, in a stochastic framework, some of the essential ingredients of mesoscale turbulence. In particular, this model fully exploits the two-component nature of mesoscale turbulence.

## 9. Mesoscale vortices and the marine ecosystem

Mesoscale and sub-mesoscale vortices play a potentially important role in the dynamics of the marine ecosystem. In particular, the presence of coherent vortices can have a significant impact on primary productivity in the open ocean (and, consequently, on the carbon cycle). Vortices induce secondary currents that can lead to upwelling and downwelling in and around the vortex. The eddy pumping mechanism (Falkowski et al 1991, McGillicuddy and Robinson 1997, McGillicuddy et al. 1998, Siegel et al. 1999) is based on the fact that isopycnals are lifted upwards, towards the surface, in cyclonic eddies. This mechanism can thus bring up nutrients from the deeper waters. In this view, cyclonic eddies act as nutrient pumps for the marine ecosystem. This view has recently been questioned by various authors (e.g., Smith et al. 1996, Lévy 2003, Williams and Follows 2003), who showed that nutrient fluxes associated with horizontal secondary circulations should be considered as well. Finally, other oceanic structures such as fronts have been suggested to be more relevant to the functioning of the marine ecosystem (Mahadevan and Archer 2000). The detailed effect of individual mesoscale eddies on the vertical fluxes of nutrients is thus currently under debate.

In any case, the work mentioned above indicates that mesoscale and sub-mesoscale structures are responsible, one way or another, for significant nutrient fluxes in the marine ecosystem. As a result, nutrient fluxes can thus be highly inhomogeneous both spatially and temporally. The fact that the nutrient supply is concentrated in small individual regions with eddy sizes rather than in a large uniform region has been shown by Martin et al. (2002) to significantly affect numerical estimates of primary productivity in the ocean.

When a fluid flow advects nutrients and plankton, the equations describing the dynamics of the biological system are advection-reaction-diffusion partial differential equations. These can be integrated in an Eulerian approach, or by a semi-Lagrangian method which copes with the dynamics of individual fluid particles. In a semi-Lagrangian numerical approach, one integrates the biological reactions in a large ensemble of Lagrangian particles which are advected by a

velocity field produced by the Eulerian integration of the momentum equations (see, e.g., Abraham 1998). Each Lagrangian parcel represents a given water volume (usually taken to have a size comparable with the Eulerian grid spacing), and it is assumed to have homogeneous properties.

In principle, the biological reactions occur within each parcel, and do not depend on the behavior of neighbouring particles. This allows for the formation of sharp gradients, when the system is prone to this behavior. When a concentration field is required, the distribution of Lagrangian particles is interpolated onto a regular grid and a concentration field is obtained. Diffusion of the biological components can be accounted for by introducing mixing among nearby water parcels (Pasquero et al., 2004).

The plankton ecosystem model used here includes three components, which represent nutrient,  $N$ , phytoplankton,  $P$ , and zooplankton,  $Z$ . The dynamics of the ecosystem is described by the NPZ equations

$$\begin{aligned}\frac{dN}{dt} &= \Phi_N - \beta \frac{N}{k_N + N} P + \\ &\quad + \mu_N \left( (1 - \gamma) \frac{a\epsilon P^2}{a + \epsilon P^2} Z + \mu_P P + \mu_Z Z^2 \right) \\ \frac{dP}{dt} &= \beta \frac{N}{k_N + N} P - \frac{a\epsilon P^2}{a + \epsilon P^2} Z - \mu_P P \\ \frac{dZ}{dt} &= \gamma \frac{a\epsilon P^2}{a + \epsilon P^2} Z - \mu_Z Z^2 .\end{aligned}\tag{15}$$

The terms on the right hand side of the equation for the nutrient represent respectively vertical nitrate supply from deep water, conversion to organic matter through phytoplankton activity, and regeneration of the dead organic matter into nutrients. The phytoplankton dynamics is regulated by production, depending on available nutrients through a Holling type-II functional response, by a Holling type III grazing by zooplankton, and by linear mortality. Finally, zooplankton grows when phytoplankton is present ( $\gamma$  is the assimilation efficiency of the zooplankton), and has a quadratic mortality term used to close the system and parameterize the effects of higher trophic levels. The specific form of the terms used in this model is quite standard in marine ecosystem modelling (Oschlies and Garcon, 1999). The term  $\mu_N$  is smaller than one and it represents the fact that not all biological substance is immediately available as nutrient: the fraction  $(1 - \mu_N)$  is lost by sinking to deeper waters. Note, also, that nutrient enters this model by affecting the growth rate of phytoplankton. Since the formulation adopted here is two-dimensional in the horizontal and no vertical structure of the fields is allowed, vertical upwelling has to be parameterized. The parameter values used in the model are listed in table 1.

The nutrient flux is expressed as a relaxation term,  $\Phi_N = -s(x, y) (N - N_0)$ , where  $N_0$  is the (constant) nutrient content in deep waters and  $s$  is the (spatially varying) relaxation rate of the nutrient, which is large in regions of strong vertical mixing and small in regions of weak vertical mixing. This form of the nutrient flux term reflects the fact that nutrient is brought up to the

---

$\beta$	$= 0.66 \text{ day}^{-1}$	$k_N$	$= 0.5 \text{ mmol N m}^{-3}$
$\epsilon$	$= 1.0 (\text{mmol N m}^{-3})^{-2} \text{ day}^{-1}$	$\mu_N$	$= 0.2$
$\gamma$	$= 0.75$	$\mu_P$	$= 0.03 \text{ day}^{-1}$
$a$	$= 2.0 \text{ day}^{-1}$	$\mu_Z$	$= 0.2 (\text{mmol N m}^{-3})^{-1} \text{ day}^{-1}$
$s$	$= s_p = 0.00648 \text{ day}^{-1}$ in nutrient-poor regions	$N_0$	$= 8.0 \text{ mmol N m}^{-3}$
$s$	$= s_a = 0.648 \text{ day}^{-1}$ in nutrient-rich regions		

---

Table 1: List of parameters used in the NPZ ecosystem models adopted here.

surface from deep water via (isopycnal and diapycnal) turbulent mixing and upwelling. This form of the nutrient flux is the standard formulation used for chemostat models when the reservoir has infinite capacity (Kot 2001).

The model ecosystem equations are solved, using the semi-Lagrangian method, for each water parcel moving in forced and dissipated, statistically stationary two-dimensional turbulence. The turbulent field used here is forced at wavenumber  $k = 40$  and has a resolution of  $512^2$  grid points (Pasquero et al. 2001; 2004). Assuming that the forcing scale corresponds to a typical eddy size, say about 25 km, then in dimensional units the domain size becomes 1000 km and the resolution is about 2 km. The turbulent velocity field has mean eddy turnover time  $T_E = 2.8$  days.

In the following, we illustrate the effect of coherent eddies on primary productivity by considering two situations which differ by the spatial distribution of the regions where the nutrient is supplied. While the total area of the “active” region with strong upwelling is kept constant at 12% of the domain area, in the first simulation the intense upwelling is confined to a circular patch at the center of the domain (case CP, Central Patch), while in the second simulation the nutrient is supplied due to upwelling in a number of small patches correlated with eddy structures (Case EP, Eddy Patches). The two types of active regions are shown in figure 3. For the EP case, the figure is a snapshot at a particular time, and the active regions are dynamically moving and changing with the flow.

In the EP case, the intense nutrient flux is assumed to take place in correspondence of the coherent vortices. The active patches with significant upwelling are defined using the value of the Okubo-Weiss parameter,  $Q = s^2 - \omega^2$  where  $s^2$  is squared strain and  $\omega^2$  is squared vorticity (Okubo 1970, Weiss 1991). The nutrient flux is defined to take place in regions for which  $|Q| > Q_0$ , where  $Q_0$  is a threshold fixed by the requirement that the total area covered by the active regions is  $12\% \pm 0.5\%$  at any time. This definition of active patches includes both the vortex cores and small annular regions around the vortices.

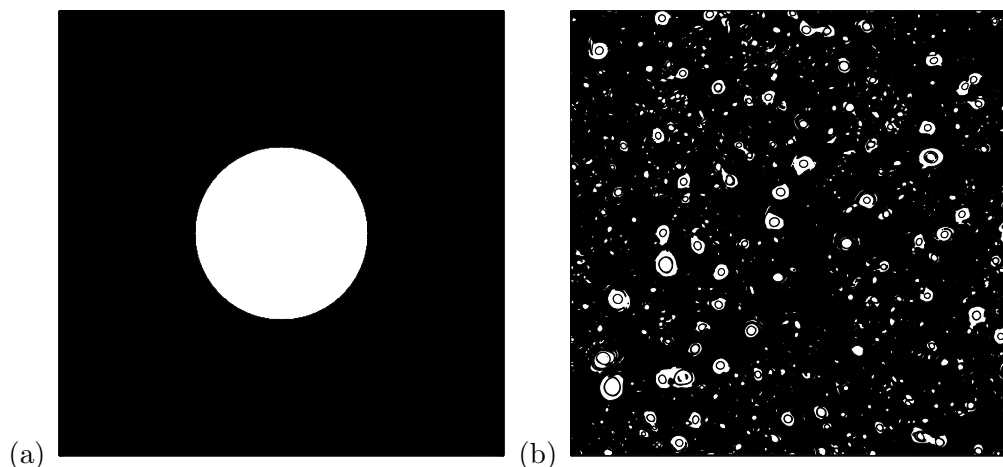


Figure 3: White areas mark the regions where intense nutrient flux takes place. Panel (a) refers to the case with a single region of strong upwelling (CP), panel (b) shows a snapshot of the case where upwelling is located in and around eddies (EP). The total area of the regions with strong upwelling is approximately the same in the two cases.

In the absence of an advecting flow and diffusion, the system reduces to an ensemble of independent, point-like (homogeneous) ecosystem models described by the system of ordinary differential equations (15). Each of these systems is labelled by the (fixed) spatial position of the corresponding fluid parcel and it is characterized by a specific value of the nutrient flux. For the parameter values adopted here, each of these systems tends to a steady state,  $(N^*, P^*, Z^*)$ , determined by the value of the nutrient input. Note that primary production in the steady state is larger than the nutrient flux, as a consequence of the fact that part of the organic nitrogen content is regenerated into nutrients (such as ammonium).

To study the system behavior in the presence of an advecting flow, we initialize the nutrient, the phytoplankton and the zooplankton in each fluid particle to the appropriate steady solution (which depends on the local value of the nutrient flux). Turbulent advection is then turned on and the evolution of the system is followed for 300 model days.

In Figure 4 we show the mean primary production, defined as  $PP = \langle \beta NP / (k_n + N) \rangle$ , where the angular brackets indicate average over the whole domain, and the ratio between primary production and nutrient upwelling flux,  $PP/\Phi_N$ , as an indicator of the efficiency of the biological model to convert inorganic into organic matter.

With the form of nutrient flux adopted here, the enhanced stirring increases the mean flux from deep waters, as seen in Fig. 4a. The enhanced flux originates at active locations when a parcel of water that has low nutrient content is advected over them. To see how this happens, consider two nearby parcels: one is in a region with small nutrient upwelling and characterized by a

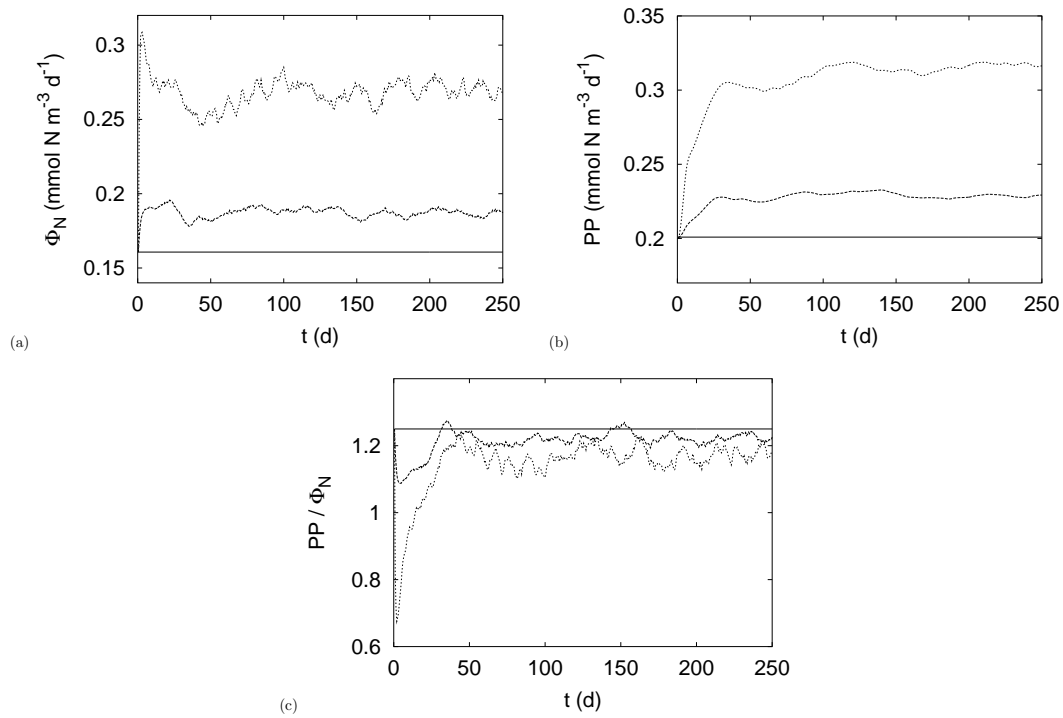


Figure 4: (a) Nitrate flux; (b) Primary productivity; (c) Primary productivity per unit nitrate flux. Solid lines show the reference case with no advection; dashed lines refer to the case with horizontal turbulent advection and nutrient flux concentrated in a single circular region (CP); dotted lines refer to the case with horizontal turbulent advection and nutrient flux distributed in small patches associated with the eddies of the turbulent flow (EP). Time is in days. [Adapted from Pasquero et al. 2004.]

steady-state nutrient concentration  $N_p^*$ ; the other is in an active region and has a steady-state nutrient concentration  $N_a^*$ . In this configuration, the total nitrate flux associated with these two parcels of water is  $(s_p(N_0 - N_p^*) + s_a(N_0 - N_a^*))$ , where  $s_p$  and  $s_a$  are the relaxation constants for the nutrient-poor and nutrient-rich regions, respectively. Suppose now that, due to advection, the two parcels switch their position: the parcel with small nutrient content gets in a strong upwelling region and vice-versa. In this configuration, the vertical flux is  $(s_p(N_0 - N_a^*) + s_a(N_0 - N_p^*))$ . The net variation of the nutrient flux between the two configurations is  $(s_a - s_p)(N_a^* - N_p^*)$ , which is proportional to  $(s_a - s_p)$ . This term is positive as larger relaxation rates are found in active regions with strong vertical mixing. The enhanced nutrient flux is thus due to the asymmetry in the relaxation times between the active and inactive regions. Note, also, that the exchange rate of water parcels between the two types of region directly affects the increased nutrient flux to the surface, determining larger values of the nutrient flux in case EP than in case CP (Fig. 4a). Primary productivity follows the increased nutrient flux, although with some delay due to the time taken by the phytoplankton to grow (Figure 4b). In case EP, a much larger primary productivity is observed than in case CP or in the absence of horizontal advection, as already observed by Martin et al. (2002). The enhanced primary productivity is due to the larger nutrient flux stimulated by the presence of horizontal advection. In fact, after the initial transient the efficiency of the biological system is about the same as in the no-advection case (Figure 4c), confirming that the primary production has increased mainly as a response to the larger available nitrate. If we had considered other forms for the nutrient flux, such as a fixed-flux condition, the results would have been somehow different, see Pasquero et al. (2004) for a comparison between different forms of the nutrient flux term. In general, however, what emerges is that the ecosystem response, for example in terms of primary productivity, is affected by the spatial and temporal fragmentation of the upwelling regions. Thus, ocean models that do not properly resolve the size of the upwelling regions, be they associated with mesoscale vortices, fronts or submesoscale structures, can provide erroneous estimates of the primary productivity of marine ecosystems.

## 10. Perspectives

In the last twenty years, we have gained some understanding of the role that mesoscale vortices play in ocean dynamics and in ocean transport processes. In particular, we have evolved from a view that considered vortices as interesting but probably irrelevant curiosities to a view of the ocean as “a sea of eddies.” Nevertheless, many issues are still open. In the following we list some of the problems (or obsessions) that capture our attention.

First, we should develop better census algorithms capable of extracting information from a few Eulerian and Lagrangian time series and of coping with inhomogeneous conditions. Up to now, vortex census algorithms either require the knowledge of the full vorticity field (Benzi et al. 1987,

Farge and Rabreau 1988, McWilliams 1990, Siegel and Weiss 1997, McWilliams et al. 1999, Farge et al. 1999) or work only for homogeneous turbulence (Pasquero et al. 2002).

Second, vortices are not the only structures present in ocean mesoscale turbulence. Rossby waves can play an important role in particle dispersion processes (e.g., Mockett 1998), and fronts are of overwhelming importance. These structures should be studied as carefully as vortices have been. An important issue, then, concerns the reason to study the effects of vortices, and of the other mesoscale structures. In our opinion, one central reason is to learn how to parameterize them. Although numerical models of the ocean circulation are attaining increasingly larger resolution, there are limits imposed by both numerical possibilities and the availability of a fine enough network of measured data for model initialization and assimilation. In such conditions, we think it is wise to devote some effort to the development of stochastic parameterizations of the effects that vortices, waves and fronts induce. The works discussed in section 8 are an example of this approach.

A much harder, but even more intriguing issue, is the stochastic parameterization of the effects that mesoscale structures have on the marine ecosystem; i.e., the parameterization of the reaction rates and of the dynamics of an ensemble of (biologically) reacting tracers. In section 9 we saw that the presence of mesoscale vortices has a direct impact on nutrient fluxes and on the primary productivity of the marine ecosystem, and an even larger impact is presumably associated with the presence of fronts. Understanding and parameterizing the biological effects of these mesoscale structures will be a major challenge in the coming years.

### **Acknowledgements**

The authors thank the Editors of this volume and two anonymous reviewers who have carefully read the manuscript and suggested how to improve it. This work was supported in part by the European Community's Human Potential Programme under contract HPRN-CT-2002-00300, Stirring and Mixing.

### **References**

- Abraham, E.R., 1998: The generation of plankton patchiness by turbulent stirring. *Nature*, **391**, 577-580.
- Arhan M., Mercier H., and Lutjeharms J.R.E., 1999: The disparate evolution of three Agulhas rings in the South Atlantic Ocean. *J. Geophys. Res. Oceans*, **104**, 20987-21005.
- Artale, V., G. Boffetta, A. Celani, M. Cencini, and A. Vulpiani, 1997: Dispersion of passive tracers in closed basins: Beyond the diffusion coefficient. *Phys. Fluids*, **9**, 3162-3171.
- Babiano, A., J.H.E. Cartwright, O. Piro, and A. Provenzale, 2000: Dynamics of small neutrally buoyant sphere in a fluid and targeting in Hamiltonian systems. *Phys. Rev. Lett.*, **84**, 5764-5767.

- Babiano, A., G. Boffetta, A. Provenzale, and A. Vulpiani, 1994: Chaotic advection in point vortex models and two-dimensional turbulence. *Phys. Fluids*, **6**, 2465-2474.
- Bauer, S., M.S. Swenson, and A. Griffa, 2002: Eddy-mean flow decomposition and eddy-diffusivity estimates in the tropical Pacific Ocean. 2. Results. *J. Geophys. Res. Ocean*, **107**, 3154-3171.
- Benzi, R., S. Patarnello, and P. Santangelo, 1987: On the statistical properties of two-dimensional decaying turbulence. *Europhys. Lett.*, **3**, 811-818.
- Berloff P.S. and J.C. McWilliams, 2002: Material transport in oceanic gyres. Part II: Hierarchy of stochastic models. *J. Phys. Oceanogr.*, **32**, 797-830.
- Berloff, P.S., J.C. McWilliams, and A. Bracco, 2002: Material transport in oceanic gyres. Part I: Phenomenology. *J. Phys. Oceanogr.*, **32**, 764-796.
- Beron-Vera, F.J., M.J. Olascoaga, M.G. Brown, 2004: Passive tracer patchiness and particle trajectory stability in incompressible two-dimensional flows. *Nonlinear Processes in Geophysics*, **11**, 67-74.
- Bower, A.S., L. Armi, and I. Ambar, 1997: Lagrangian observations of Meddy formation during a mediterranean undercurrent seeding experiment. *J. Phys. Oceanogr.*, **27**, 2545-2575.
- Bracco, A., J. LaCasce, C. Pasquero, and A. Provenzale, 2000a: The velocity distribution of barotropic turbulence. *Phys. Fluids*, **12**, 2478-2488.
- Bracco, A., J.H. LaCasce, and A. Provenzale, 2000b: Velocity probability density functions for oceanic floats. *J. Phys. Oceanogr.*, **30**, 461-474.
- Bracco, A., A. Provenzale, and I. Scheuring, 2000c: Mesoscale vortices and the paradox of the plankton. *P. Roy. Soc. Lond. B*, **267**, 1795-1800.
- Bracco, A., E.P. Chassignet, Z.D. Garraffo, A. Provenzale, 2003: Lagrangian velocity distributions in a high-resolution numerical simulation of the North-Atlantic. *J. Atmos. Ocean. Tech.* **20**, 1212-1220.
- Bracco, A., J. von Hardenberg, A. Provenzale, J.B. Weiss, and J.C. McWilliams, 2004: Dispersion and mixing in quasigeostrophic turbulence. *Phys. Rev. Lett.*, **92**, 084501.
- Brickman D. and P.C. Smith, 2002: Lagrangian stochastic modeling in coastal oceanography. *J. Atmos. Ocean. Tech.*, **19**, 83-99.
- Brown, M.G. and K.B. Smith, 1990: Are SOFAR Float Trajectories Chaotic? *J. Phys. Oceanogr.*, **20**, 139-149.
- Colin de Verdiere A., 1983: Lagrangian Eddy statistics from surface drifters in the eastern North-Atlantic. *J. Marine Res.*, **41**, 375-398.

- de Steur L, van Leeuwen P.J., and Drijfhout S.S., 2004: Tracer leakage from modeled Agulhas rings. *J. Phys. Oceanogr.*, **34**, 1387-1399.
- Elhmaidi, D., A. Provenzale, and A. Babiano, 1993: Elementary topology of two-dimensional turbulence from a Lagrangian viewpoint and single-particle dispersion. *J. Fluid Mech.*, **242**, 655-700.
- Falco, P., A. Griffa, P.M. Poulain, and E. Zambianchi, 2000: Transport properties in the Adriatic Sea as deduced from drifter data. *J. Phys. Oceanogr.*, **30**, 2055-2071.
- Falkowski, P.G., D. Ziemann, Z. Kolber, and P.K. Bienfang, 1991: Role of eddy pumping in enhancing primary production in the Ocean. *Nature*, **352**, 55-58.
- Farge, M. and G. Rabreau, 1988: Wavelet transform to detect and analyze coherent structures in two-dimensional turbulent flows. *C. Acad. Sci. Paris Sér. II*, **307**, 1479-1486.
- Farge, M., K. Schneider, and N. Kevlahan, 1999: Non-Gaussianity and coherent vortex simulation for two-dimensional turbulence using an adaptive orthogonal wavelet basis. *Phys. Fluids*, **11**, 2187-2201.
- Flierl, G.R., 1987: Isolated eddy models in geophysics. *Ann. Rev. Fluid Mechanics*, **19**, 493-530.
- Garraffo, Z.D., A.J. Mariano, A. Griffa, C. Veneziani, and E.P. Chassignet, 2001: Lagrangian data in a high-resolution numerical simulation of the North Atlantic I. Comparison with in situ drifter data. *J. Marine Syst.*, **29**, 157-176.
- Garzoli S.L., Richardson P.L., Rae C.M.D., Fratantoni D.M., Goni G.J., and Roubicek A.J., 1999: Three Agulhas rings observed during the Benguela Current experiment. *J. Geophys. Res. Oceans*, **104**, 20971-20985.
- Goni G.J., Garzoli S.L., Roubicek A.J., Olson D.B., and Brown O.B., 1997: Agulhas ring dynamics from TOPEX/POSEIDON satellite altimeter data. *J. Marine Res.*, **55**, 861-883.
- Griffa, A., 1996: Applications of stochastic particle models to oceanographic problems. In *Stochastic Modelling in Physical Oceanography* (ed. R.J. Afler, P. Müller, & R.B. Rozovskii), pp. 114-140.
- Griffa, A., K. Owens, L. Piterbarg, and B. Rozovskii, 1995: Estimates of turbulence parameters from Lagrangian data using a stochastic particle model. *J. Marine Res.*, **53**, 371-401.
- Hogg N.G. and W.B. Owens, 1999: Direct measurement of the deep circulation within the Brazil Basin. *Deep-sea Res. Part II*, **46**, 335-353.
- Hooker S.B. and J.W. Brown, 1995: Warm-core ring dynamics derived from satellite imagery. *J. Geophys. Res. Oceans*, **99**(C12), 25181-25194.
- Isern-Fontanet, J., E. Garcia-Ladona, and J. Font, 2003: Identification of marine eddies from altimetric maps. *J. Atmos. Ocean. Tech.*, **20**, 772-778.

- Jiménez, J., 1996: Algebraic probability density tails in decaying isotropic two-dimensional turbulence. *J. Fluid Mech.*, **313**, 223-240.
- Kot, M., 2001: Elements of Mathematical Ecology. *Cambridge Univ. Press*, 464pp.
- Lévy, M., 2003: Mesoscale variability of phytoplankton and of new production: Impact of the large-scale nutrient distribution. *J. Geophys. Res. Oceans*, **108**(C11), 3358.
- Lévy, M., P. Klein, and A.M. Tréguier, 2001: Impact of sub-mesoscale physics on production and subduction of phytoplankton in an oligotrophic regime. *J. Marine Res.*, **59**, 535-565.
- Mahadevan A. and D. Archer, 2000: Modeling the impact of fronts and mesoscale circulation on the nutrient supply and biogeochemistry of the upper ocean. *J. Geophys. Res. Oceans*, **105**, 1209-1225.
- Mahadevan A. and J.W. Campbell, 2002: Biogeochemical patchiness at the sea surface. *Geophys. Res. Lett.*, **29**, 1926.
- Mann K.H. and J.R.N. Lazier, 1996: Dynamics of marine ecosystems: Biological-Physical interactions in the Oceans, 2nd ed. *Blackwell Science, Cambridge, MA*.
- Martin, A.P., K.J. Richards, A. Bracco, and A. Provenzale, 2002: Patchy productivity in the open ocean. *Global Biogeochem. Cycles*, **16**, 1025.
- Martin A.P. and K.J. Richards, 2001: Mechanisms for vertical nutrient transport within a North Atlantic mesoscale eddy. *Deep-sea Res. Part II*, **48**, 757-773.
- Martin, A.P., 2003: Phytoplankton patchiness: the role of lateral stirring and mixing. *Progress in Oceanography*, **57**, 125.
- Maurizi, A., A. Griffa, P.M. Poulain, and F. Tampieri, 2004: Lagrangian turbulence in the Adriatic Sea as computed from drifter data: Effects of inhomogeneity and nonstationarity. *J. Geophys. Res. Oceans*, **109**, C04010.
- McGillicuddy D.J. and A.R. Robinson, 1997: Eddy-induced nutrient supply and new production in the Sargasso Sea. *Deep-sea Res. Part I*, **44**, 1427-1450.
- McGillicuddy, D.J., A.R. Robinson, D.A. Siegel, H.W. Jannasch, R. Johnson, T. Dickey, J. McNeil, A.F. Michaels, A.H. Knap, 1998: Influence of mesoscale eddies on new production in the Sargasso Sea. *Nature*, **394**, 263-266.
- McIntyre, M.E., 1989: On the Antarctic ozone hole. *J. Atmos. Terr. Phys*, **51**, 29-43.
- McWilliams, J.C., 1985: Submesoscale, coherent vortices in the ocean. *Rev. Geophys.*, **23**, 165-182.
- McWilliams, J.C., 1990: The vortices of two-dimensional turbulence. *J. Fluid Mech.*, **219**, 361-385.

- McWilliams, J.C., J.B. Weiss, and I. Yavneh, 1999: The vortices of homogeneous geostrophic turbulence. *J. Fluid Mech.*, **401**, 1-26.
- Min, I.A., I. Mezic, A. Leonard, 1996: Levy stable distributions for velocity difference in systems of vortex elements. *Phys. Fluids*, **8**, 1169-1180.
- Mockett, C.R., 1998: Dispersion and Reconstruction. In *Astrophysical and Geophysical Flows as Dynamical System*, WHOI Tech. Rep. WHOI-98-00.
- Okubo, A., 1970: Horizontal dispersion of floatable particles in the vicinity of velocity singularities such as convergences. *Deep-sea Res.*, **17**, 445-454.
- Olson, D.B., 1991: Rings in the ocean. *Annu. Rev. Earth. Planet. Sci.*, **19**, 133-183.
- Olson, D.B., and R.H. Evans, 1986: Rings of the Agulhas Current. *Deep-sea Res. Part A*, **33**, 27-42.
- Osborne, A.R., A.D. Kirwan, A. Provenzale, and L. Bergamasco, 1986: A search for chaotic behavior in large and mesoscale motions in the Pacific Ocean. *Physica D*, **23**, 75-83.
- Osborne, A.R., A.D. Kirwan, A. Provenzale, and L. Bergamasco, 1989: Fractal drifter trajectories in the Kuroshio extension. *Tellus*, **41A**, 416-435.
- Oschlies A. and V. Garçon, 1999: An eddy-permitting coupled physical-biological model of the North Atlantic - 1. Sensitivity to advection numerics and mixed layer physics. *Global Biogeochem. Cy.*, **13**, 135-160.
- Pasquero, C., A. Bracco, and A. Provenzale, 2004: Coherent vortices, Lagrangian particles and the marine ecosystem. In *Shallow Flows*, edited by G.H. Jirka and W.S.J. Uijttewaal, Balkema Publishers, Leiden, NL, 399-412.
- Pasquero, C., A. Provenzale, and J.B. Weiss, 2002: Vortex statistics from Eulerian and Lagrangian time series. *Phys. Rev. Lett.*, **89**, 284501.
- Pasquero, C., A. Provenzale, and A. Babiano, 2001: Parameterization of dispersion in two-dimensional turbulence. *J. Fluid Mech.*, **439**, 279-303.
- Pedlosky, J., 1987: Geophysical Fluid Dynamics. *Springer, 2nd ed.*, 710pp.
- Pickart, R.S., W.M. Smethie, J.R.N. Lazier, E.P. Jones, and W.J. Jenkins, 1996: Eddies of newly formed upper Labrador Sea water. *J. Geophys. Res. Oceans*, **101**(C9), 20711-20726.
- Poulain, P.M., 2001: Adriatic Sea surface circulation as derived from drifter data between 1990 and 1999. *J. Marine Syst.*, **29**, 3-32.
- Provenzale, A., A.R. Osborne, A.D. Kirwan, and L. Bergamasco, 1991: The study of fluid parcel trajectories in large-scale ocean flows. In *Nonlinear Topics in Ocean Physics*, edited by A.R. Osborne (Elsevier, Amsterdam), 367-401.

- Provenzale, A., 1999: Transport by coherent barotropic vortices. *Annu. Rev. Fluid Mech.*, **31**, 55-93.
- Reynolds, A.M., 2002: On Lagrangian stochastic modelling of material transport in oceanic gyres. *Physica D*, **172**, 124-138.
- Richardson P.L., 1993: A census of eddies observed in North-Atlantic SOFAR float data. *Progress in Oceanography*, **31**, 1-50.
- Richardson, P.L., A.S. Bower, and W. Zenk, 2000: A census of Meddies tracked by floats. *Progress in Oceanography*, **45**, 209-250.
- Richardson, P.L., G.E Hufford, R. Limeburner, and W.S. Brown, 1994: North Brazil current retroflection eddies. *J. Geophys. Res. Oceans*, **99**, 5081-5093.
- Richardson P.L. and D.M. Fratantoni, 1999: Float trajectories in the deep western boundary current and deep equatorial jets of the tropical Atlantic. *Deep-sea Res. Part II*, **46**, 305-333.
- Rodean, H.C., 1996: Stochastic Lagrangian models of turbulent diffusion. *Meteor. Monographs*, **26**(48), 84pp.
- Rupolo, V., B.L. Hua, A. Provenzale, V. Artale, 1996: Lagrangian velocity spectra at 700m in the western North Atlantic. *J. Phys. Oceanogr.*, **26**, 1591-1607.
- Salmon R., 1998: Lectures on Geophysical Fluid Dynamics. *Oxford Univ. Press*, 378pp.
- Sanderson, B.G. and D.A. Booth, 1991: The fractal dimension of drifter trajectories and estimates for horizontal eddy-diffusivity. *Tellus*, **43A**, 334-349.
- Sawford, B.L., 1999: Rotation of trajectories in lagrangian stochastic models of turbulent dispersion. *Bound.-Lay. Meteorol.*, **93**, 411-424.
- Shapiro G.I. and S.L. Meschanov, 1991: Distribution and spreading of Red-Sea water and salt lens formation in the Northwest Indian-Ocean. *Deep-sea Res. Part A*, **38**, 21-34.
- Siegel, A. and J.B. Weiss, 1997: A wavelet-packet census algorithm for calculating vortex statistics. *Phys. Fluids*, **9**, 1988-1999.
- Siegel, D., D.J. McGillicuddy, and E.A. Fields, 1999: Mesoscale eddies, satellite altimetry, and new production in the Sargasso Sea. *J. Geophys. Res. Oceans*, **104**(C6), 13359-13379.
- Smith, C.L., K.J. Richards, and M.J.R. Fasham, 1996: The impact of mesoscale eddies on plankton dynamics in the upper ocean. *Deep-sea Res. II*, **1807-1832**.
- Stammer D., 1997: Global characteristics of ocean variability estimated from regional TOPEX/POSEIDON altimeter measurements. *J. Phys. Oceanogr.*, **27**, 1743-1769.
- Testor P. and J.C. Gascard, 2003: Large-scale spreading of deep waters in the Western Mediterranean sea by submesoscale coherent eddies. *J. Phys. Oceanogr.*, **33**, 75-87.

- Thomson, D.J., 1987: Criteria for the selection of stochastic models of particle trajectories in turbulent flows. *J. Fluid Mech.*, **180**, 529-556.
- Veneziani, M., A. Griffa, A.M. Reynolds, A.J. Mariano, 2004: Oceanic turbulence and stochastic models from subsurface Lagrangian data for the northwest Atlantic Ocean. *J. Phys. Oceanog.*, **34**, 1884-1906.
- Weatherly, G., M. Arhan, H. Mercier, and W. Smethie, 2002: Evidence of abyssal eddies in the Brazil Basin. *J. Geophys. Res. Oceans*, **107**(C4), 3027.
- Weiss, J.B., 1991: The dynamics of enstrophy transfer in two-dimensional hydrodynamics. *Physica D*, **48**, 273-294.
- Weiss, J.B., A. Provenzale, J.C. McWilliams, 1998: Lagrangian dynamics in high-dimensional point-vortex systems. *Phys. Fluids*, **10**, 1929-1941.
- Williams R.G. and M.J. Follows, 2003: Physical transport of nutrients and the maintenance of biological production. In *Ocean biogeochemistry The role of the ocean carbon cycle in global change* (ed. by M. Fasham) 19-51.
- Zhang, H. M., M.D. Prater, and T. Rossby, 2001: Isopycnal Lagrangian statistics from the North Atlantic current RAFOS float observations. *J. Geophys. Res. Oceans*, **106**, 13817-13836.